Taking monocrystalline silicon to the ultimate lifetime limit

T. Niewelt[a,b,*], A. Richter[a], T.C. Kho[c], N.E. Grant[d], R.S. Bonilla[e], B. Steinhauser[a], J.-I. Polzin[a,b], F. Feldmann[a,b], M. Hermle[a], J.D. Murphy[d], S.P. Phang[c], W. Kwapil[a,b], M.C. Schubert[a]

[a] Fraunhofer Institute for Solar Energy Systems ISE, Freiburg, Germany
[b] Laboratory for Photovoltaic Energy Conversion and Freiburg Materials Research Centre FMF, University of Freiburg, Freiburg, Germany
[c] Research School of Engineering, The Australian National University, Canberra, Australia
[d] School of Engineering, University of Warwick, Coventry CV4 7AL, United Kingdom
[e] Department of Materials, University of Oxford, Oxford OX1 3PH, United Kingdom

ABSTRACT

A central quantity to assess the high quality of monocrystalline silicon (on scales beyond mere purity) is the minority charge carrier lifetime. We demonstrate that the lifetime in high purity float zone material can be improved beyond existing observations, thanks to a deeper understanding of grown-in defects and how they can be permanently annihilated. In a first step we investigate the influence of several process sequences on the lifetime by applying a low temperature superacid passivation treatment. We find that a pre-treatment consisting of an oxidation at 1050 °C followed by a POCl$_3$ diffusion at 900 °C can improve the lifetime by deactivating or eliminating grown-in defects. Then, pre-treated wafers of different float zone materials are passivated with three state-of-the-art layer stacks. Very high effective lifetime values are measured, thereby demonstrating the high quality of the surface passivation schemes and the pre-treated silicon wafers. The measured effective lifetimes exceed previous records, and we report an effective lifetime of 225 ms measured on a 200 μm thick 100 Ω cm n-type silicon wafer symmetrically passivated with a layer stack of a thin thermally grown oxide and a poly-crystalline layer (the TOPCon layer stack).

1. Introduction

In the recent years the photovoltaic community has seen significant improvements in the efficiency of both industrially produced solar cells and record efficiencies of elaborate research scale cells, e.g. [1–3]. A major share of this development is due to ongoing improvements in surface passivation strategies and process advancements to utilise the high electrical quality of today's silicon wafers. This high quality has in turn been achieved by improvement of crystallization technologies (e.g. [4]) and optimised process routes that deactivate recombination-active bulk defects in commercially feasible material (e.g. [5–7]).

Float zone (FZ) silicon wafers are commonly used as a reference to study dielectric surface passivation, intrinsic recombination in silicon, and the performance limit of device structures. FZ silicon is typically assumed to be virtually free of recombination-active bulk defects, and thus it is the gold standard material to measure the maximum attainable effective charge carrier lifetimes τ_{eff} and assess the influence of surface recombination. However, this assumption is weakened by the finding that FZ wafers are often affected by bulk defects introduced during crystal growth or typical sample fabrication, e.g. [8,9]. The yet

unpredictable occurrence of the defects introduces experimental scatter and can reduce reproducibility. The underlying defects are known to be affected by thermal treatments and thus distort the comparability of different process schemes due to different thermal budget [8,10]. Such unexpected changes of the bulk lifetime during processing, including dielectric deposition and subsequent annealing, can hinder the optimization of surface passivation layers, the quantification of intrinsic recombination in silicon and loss analyses in high performance solar cells.

In order fairly to compare advancements in surface passivation, the underlying bulk material must be well understood and it's bulk lifetime τ_{bulk} reliably obtained. FZ silicon provides a means to achieve this. However in moving forward, the PV industry must take into consideration, that depending on very specific growth conditions, different FZ silicon wafers of the same resistivity (i.e. different manufacturers) can feature significantly different τ_{bulk}. Fortunately, the grown-in defects responsible for this effect can be annihilated by high temperature processing [8], which in principle, will provide a means to quantify surface passivation quality accurately.

In this contribution we demonstrate that common thermal

---

treatments can be used to improve the bulk lifetime of various typical FZ silicon materials. A recently developed superacid passivation treatment [11] is applied to wafers after different processes to demonstrate their impact on the wafer bulk. We suggest a process sequence that deactivates the bulk defects and transfers FZ silicon wafers to a stable state. FZ wafers should undergo such pre-treatment before the application as reference substrates. To support this suggestion the treatment is applied to a range of different FZ materials that are subsequently passivated with state-of-the-art surface passivation layers. The sample processing is performed at two institutes on wafers of the same material to demonstrate that the process sequence allows a direct comparison of passivation layers. We present record lifetimes on all investigated materials. This indicates that the pre-treatment improved the quality of the bulk material and demonstrates the quality of the surface passivation processes.

2. Sample processing

The investigated FZ silicon wafers from commercial suppliers represent a typical quality level used in photovoltaic research. The materials were chosen to cover a large doping concentration range and feature both p- and n-type doping. The specifications of the investigated materials are listed in Table 1. Exact resistivities were measured using the Van der Pauw technique [12] in rectangular $5 \times 5 \, mm^2$ samples cut off one wafer after the experiments had been completed. The wafers of each material originate from the same box or batch to make sure that they originate from the same FZ crystal for best comparability. The three performed experiments are discussed in the following subsections and summarised in Fig. 1. The experiments were performed on full 4″ wafers, unless stated otherwise.

2.1. Experiment 1: influence of processes on the bulk lifetime

We investigated the influence of the following processes on the bulk lifetime τ_{bulk} of FZ Si wafers:

Pre-treatments:

– POCl$_3$ diffusion gettering in a quartz tube furnace

(60 min at 900 °C, resulting P-doped regions ($R_{sheet} \approx 18 \, \Omega/\square$) etched off)

– Thermal oxidation in a quartz tube furnace

(60 min at 1050 °C, resulting oxide layer ($t_{ox} \approx 105 \, nm$) etched off)

Passivation processes:

– Al$_2$O$_3$ passivation
(plasma-assisted ALD of 20 nm Al$_2$O$_3$ on both sides at 180 °C in an Oxford Instruments OpAL reactor followed by a 25 min 440 °C forming gas anneal, see [13] for more details)
– ONO-passivation
(thermal oxidation at 1000 °C in a quartz tube furnace followed by PECVD deposition of SiN$_x$ and SiO$_x$ at/below 400 °C, see [14] for

more details).

Several combinations of sequential application of these processes were investigated on materials A-F. Sequences featuring dielectric passivation were assessed via τ_{eff} measurements and photoluminescence imaging (PLI). To assess the impact on τ_{bulk} more directly and investigate process sequences without dielectric passivation, further investigations were performed on material E. Wafers of material E in the as-grown state and after different process sequences were cleaved to quarters and subsequently etched back to bare silicon. Then, the samples were all passivated with the same passivation. Using this approach the relative comparison of τ_{eff} is sufficient to assess τ_{bulk} changes, because all sister samples feature similar surface recombination. The passivation after etching was realised via immersion in a superacid (non-aqueous solution of bis(trifluoromethane)sulfonimide (TFSI) in dichloroethane (DCE)). This treatment allows for a most direct comparison of the material quality as it provides an effective surface passivation with negligible thermal budget and no relevant introduction of hydrogen to the bulk. The process and its features are discussed in more detail in [11].

2.2. Experiment 2: direct comparison of different dielectric passivation schemes

Suitably chosen processing sequences provide FZ wafers with high and stable bulk lifetimes. While an improvement in the bulk lifetime by introducing mobile species (i.e.hydrogen) and associated thermal budgets are important features of modern processing conditions (cf. the introduction of hydrogen from [15] or impurity gettering to [16] a-SiN$_x$ layers) they can superpose the actual surface passivation quality. If achieved τ_{eff} or extracted parameters (such as saturation currents J_0 or surface recombination velocities S_0) are directly compared every unnoticed change of τ_{bulk} distorts the result. Therefore, a direct comparison of different surface schemes can only be fair, if they are applied to stable material. Based on the results of Experiment 1 the wafers underwent a pre-treatment consisting of an oxidation step at 1050 °C and a subsequent POCl$_3$ diffusion at 900 °C prior to passivation.

We processed samples to compare the performance of

A) 20 nm of ALD-Al$_2$O$_3$ (processed at Fraunhofer ISE as specified above and in [13])
B) the passivation ONO stack (processed at ANU as specified above and in [14])

on materials A-F listed in Table 1. The samples were subjected to photoluminescence imaging to check for lateral inhomogeneities that could severely affect the measured τ_{eff} (cf. [17,18]). Lifetime measurements using Sinton Instruments WCT-120 lifetime testers in transient mode were repeated on the same samples at multiple institutes for an inter laboratory comparison to assess reproducibility.

Kho et al. report that the passivation performance of ONO layer stacks can be improved further via corona charging [14]. Therefore, the samples passivated with ONO layer stacks were subjected to an enhancement procedure using corona discharge at University of Oxford. A point-to-plain set up with a steel pin at 30 kV was used to deliver

Table 1
Investigated FZ materials.

Material	A	B	C	D	E	F*	P1	N1
dopant species	B	B	P	P	P	P	B	P
nominal resistivity (Ω cm)	0.5	100	1.5	5	10	100	1	1
measured resistivity (Ω cm)	0.48 ± 0.02	107.9 ± 4	1.77 ± 0.07	4.97 ± 0.2	8.93 ± 0.35	86.7 ± 3.4	–	–
nominal thickness (μm)	400	250	400	400	200	300*	250	200

* The material F samples passivated with TOPCon originate from the same crystal but are 200 μm thick.
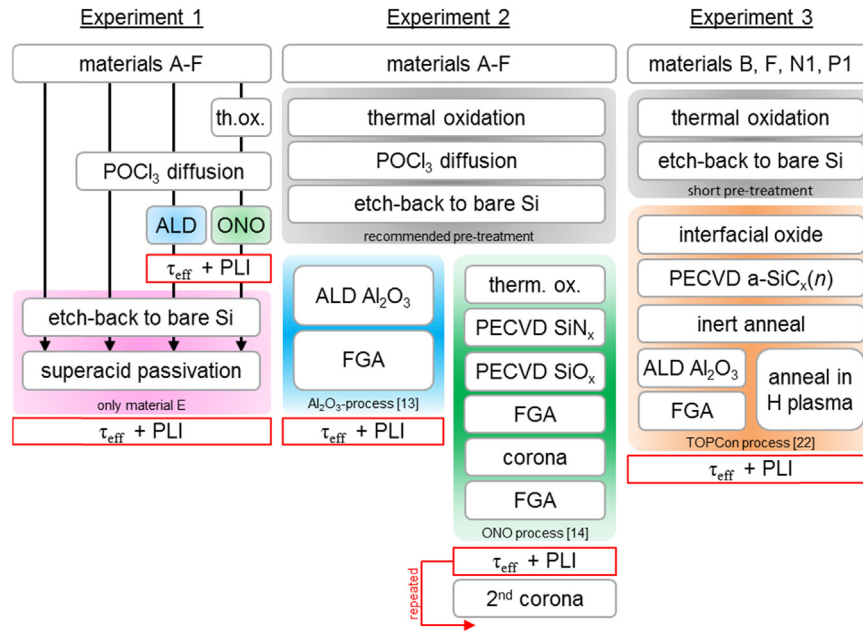
Fig. 1. Schematic process flows of the experiments. Experiment 1 was discussed in Section 2.1, Experiment 2 in Section 2.2 and Experiment 3 in Section 2.3. Further process details are specified in the given references.
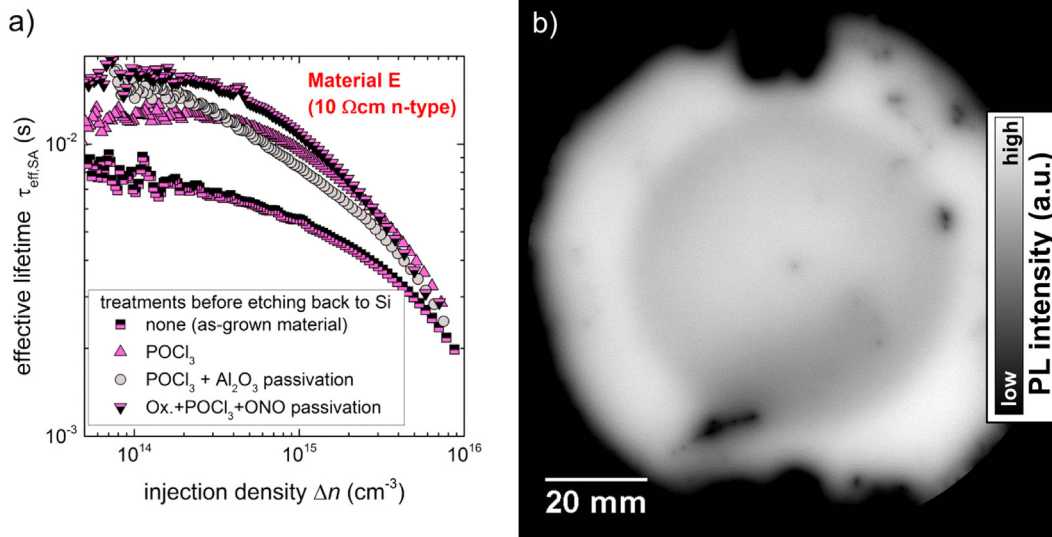

Fig. 2. a) Influence of different process sequences on τ_{bulk} (10 Ω cm n-type FZ silicon) as demonstrated by the superacid based passivation experiment. b) PL image taken at 0.05 sun equivalents illumination of a wafer from material E after POCl₃ diffusion and Al₂O₃ passivation but before the etching to bare silicon. The round feature in the wafer centre indicates a τ_{eff} limitation due to bulk defects.

4×10^{12} q/cm² uniformly to both sides of the wafer [19]. This demonstrated the high silicon bulk quality achieved with the thermal pre-treatments for samples featuring maximum τ_{eff}. Surface charge stabilisation was achieved by using a hexamethyldisilazane (HMDS) coating as reported in [20,21], such that specimens could be sent for measurements at different institutes.

2.3. Experiment 3: application of the TOPCon layer stack to lifetime samples

Recent experimental results at Fraunhofer ISE have demonstrated outstanding results when the TOPCon layer stack (tunnel oxide passivating contacts) was applied to bare FZ silicon wafers to create symmetric lifetime samples [22]. Therefore, we continued the optimization of the TOPCon layer stack for the application as a passivation scheme.

We did not apply the full pre-treatment used for Experiment 2 because the process variations we wanted to compare were rather similar. Furthermore, there has been indications in literature that polycrystalline layers similar to those applied in the TOPCon layer stack can also provide impurity gettering [23,24]. Therefore, the wafers were only oxidised at 1050 °C for 80 min to stabilise the bulk prior to the TOPCon process.

We investigated wafers of 1 and 100 Ω cm resistivity and both doping types. The p- and n-type wafers featured nominal thicknesses of 250 and 200 μm, respectively (specified in Table 1). The oxide layer resulting from the pre-treatment was etched off in a buffered oxide etch. Then, the wafers were passivated on both sides with a TOPCon process as described in [22]. This specific TOPCon stack consists of a thermally grown interfacial oxide layer and a Si-rich a-SiCₓ(n) layer deposited in a cPLASMA PECVD tool. After the deposition, the samples

were annealed in a tube furnace in inert ambient at 900 or 910 °C. Finally, the samples received a hydrogenation treatment. The hydrogenation was realised either with a tube furnace process at 400 °C in a hydrogen atmosphere [25] or with an ALD Al_2O_3 layer ontop the TOPCon stack acting as hydrogen source during a forming gas anneal at 425 °C.

3. Results

3.1. Experiment 1: influence of processes on the bulk lifetime

The results of Experiment 1 to assess the influence of the used processes on τ_{bulk} are shown in Fig. 2(a). They were obtained by using the superacid immersion passivation on material E but are representative for all materials investigated in this study. These measurements confirmed that bulk defects in the as-grown state do limit the bulk lifetime, as indicated by moderate $\tau_{eff,SA}$ (subscript $_{SA}$ indicates τ_{eff} measured with superacid passivation) on samples investigated without any thermal processing after wafer purchase. The level of $\tau_{eff,SA}$ improved after the $POCl_3$ diffusion step performed at 900 °C.

The samples that were subjected to a $POCl_3$ diffusion and subsequently passivated by Al_2O_3 (including the forming gas anneal) also show an improved $\tau_{eff,SA}$, however the injection dependence does provide some evidence of bulk recombination centres. To elucidate this finding, PL images were acquired from Al_2O_3 passivated wafers of materials A-F which underwent a $POCl_3$ diffusion pre-treatment. Fig. 1(b) shows one such PL image of material E which highlights the occurrence of a weak, but characteristic recombination ring pattern resembling the findings in [8,10]. In contrast, process flows that included a thermal oxidation and a $POCl_3$ diffusion resulted in higher $\tau_{eff,SA}$. Furthermore, such wafers did not feature any ring like recombination patterns in PL images, indicating that the combination of processes permanently annihilated the grown-in defects (not shown), which is consistent with [8]. These results underline the importance of appropriate sample processing sequences in order to achieve maximum lifetimes even in FZ material of highest quality.

3.2. Experiment 2: direct comparison of different dielectric passivation schemes

We have observed extraordinary performance of both investigated surface schemes in this experiment. The measured τ_{eff} curves were among the highest measured for comparable material resistivities at the contributing institutes. The best measured lifetime curves reached on materials A-F (cf. Table 1) with dielectric passivation layers are shown in Fig. 3 along with a comparison to the Richter parametrisation for intrinsic recombination $\tau_{intr,Richter}$ according to [26]. The measured τ_{eff} of several samples reach or even exceed the $\tau_{intr,Richter}$ limit. As no correction for surface recombination has been performed this demonstrates their outstanding quality.

The figure also contains a comparison of measurements on the best samples passivated with the ONO stack at three of the contributing institutes (faint symbols). We observe that the measured overall lifetime level shows excellent agreement. However, we observed that a stronger lifetime decline at injection levels $\Delta n > 10^{15}$ cm^{-3} was found in measurements at some institutes. At this time, we cannot distinguish whether this is due to measurement artefacts or changes of the samples due to storage and handling.

In accordance with previous results we observe an improvement of the surface passivation after corona charging reflected in an increase in τ_{eff} [14,19,21,27]. Fig. 4 illustrates the injection dependent effective lifetime for the highest τ_{eff} specimens passivated with the ONO stack, before and after corona discharge. In all cases an improvement of the lifetime is observed in the mid to high injection regimes. The overall improvement is stronger for the samples featuring lower resistivity and only slight improvement is observed for 100 Ωcm samples with the p-

type sample (material B) even showing degradation of τ_{eff} for $\Delta n < 3\cdot10^{14}$ cm^{-3} after the charge deposition. The general injection dependence of $\tau_{eff}(\Delta n)$, however, is maintained for all samples before and after corona discharge enhancement. This increase in τ_{eff} demonstrates that further improvements in the passivation quality may still be possible, and that the improvement in bulk intrinsic lifetime via pretreatment is even higher than was shown by the results in Fig. 3.

3.3. Experiment 3: lifetime samples with TOPCon layer passivation

Lifetime measurements on the samples featuring TOPCon layers as surface passivation resulted in outstanding levels of τ_{eff} on both p- and n-type material. This was achieved despite omission of the $POCl_3$ diffusion pre-treatment and the comparably small wafer thickness of the 250 and 200 μm, respectively. Wafers of both investigated resistivities featured unexpectedly high τ_{eff} values. The best measured τ_{eff} curves are shown in Fig. 5 along with indications of the extracted maxima and the Richter parametrisation of intrinsic recombination [26].

4. Discussion

The experiments demonstrate that the process sequences have an impact on the achieved lifetime level that goes way beyond the mere surface passivation quality. We combine high quality FZ Si wafers after a treatment to open up their full potential with state-of-the-art surface passivation schemes and thereby achieve very high effective charge carrier lifetimes.

4.1. Pre-treatment

As demonstrated with Experiment 1 (Section 3.1), τ_{bulk} changes significantly even during a $POCl_3$ diffusion process to which FZ silicon is generally assumed to be invariant. Gettering of impurities or reconfiguration of defects during oxidation treatments are common in less pure silicon grown via the Czochralski process or directional growth casting but would not be expected for high quality FZ silicon. We attribute the lifetime improvement to the dissolution of bulk defects or interaction of intrinsic defects (cf. [8,10]) rather than to an effect of impurity gettering. However, if metallic contaminants were present in the material it is likely that their concentration was reduced further by gettering in the phosphorus glass and/or the P-diffused region. The observed patterns (e.g. in Fig. 2b)) are indicative of an involvement of grown-in intrinsic defects (i.e. vacancies or self-interstitials) [29]. This indicates that the $POCl_3$ diffusion process did not permanently annihilate the grown-in defects. The small difference of the measured $\tau_{eff,SA}$ when comparing the sample after $POCl_3$ diffusion to the one featuring subsequent Al_2O_3 deposition and forming gas anneal indicates that τ_{bulk} did not change significantly during the passivation process.

Further improvement of $\tau_{eff,SA}$ when compared to samples after $POCl_3$ diffusion was observed for samples whose process sequences included an oxidation process. This further indicates that the $POCl_3$ diffusion step did not remove all bulk defects although the samples underwent a thermal process at 900 °C, as suggested in literature [30]. From our results we cannot determine the mechanism(s) that deactivated further bulk defects during the oxidation treatment. It is possible that this was,

I) due to interaction with species introduced during the oxidation (e.g. Si_i),
II) an effect of the higher peak temperature (1050 °C instead of 900 °C) of the process, or
III) caused by the additional processing time at high temperature.

Our findings [8,10] and literature [30] indicate that no reactivation of bulk defects with successive thermal treatments occurs after their deactivation. Therefore we have no reason to expect a change of the
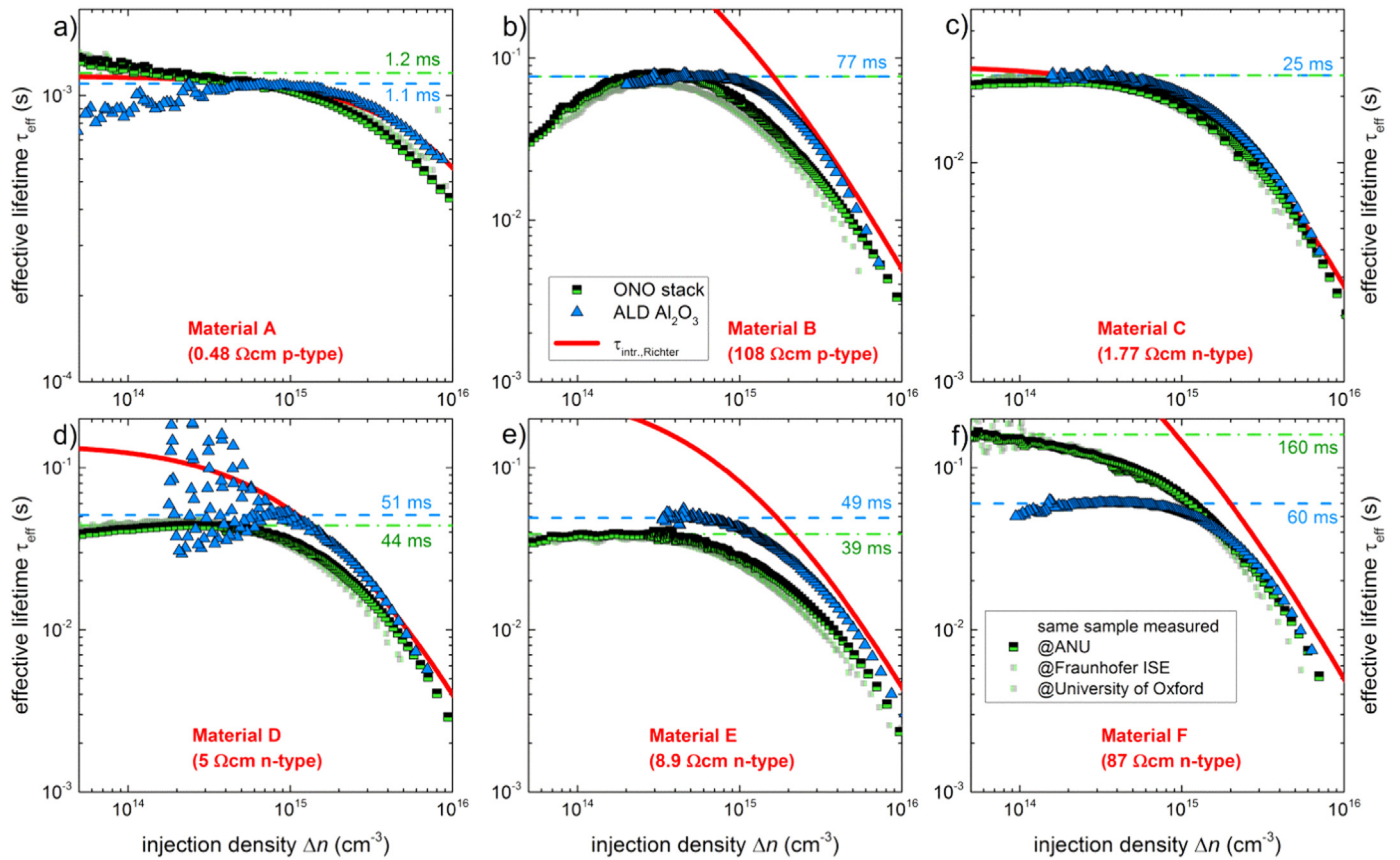
Fig. 3. Injection dependent τ_{eff} curves of the best samples of materials A-F passivated with the ONO stack (green squares) or ALD Al_2O_3 layers (blue triangles). It should be noted that some curves reach or even exceed the intrinsic lifetime limit parametrisation by Richter et al. [26] (solid red lines, evaluated for nominal material resistivity) despite being uncorrected for surface recombination. The dashed lines indicate the extracted maximum lifetimes used for Fig. 6. The faint symbols indicate measurements performed on the same samples at different institutes.

electrical quality of the bulk silicon with subsequent thermal processing and assume τ_{bulk} to be stable after the treatment including both $POCl_3$ diffusion and the oxidation treatment.

The results of Experiment 3 demonstrate that excellent lifetimes can also be achieved with a shortened version of the pre-treatment featuring only an oxidation at 1050 °C. However, it should be kept in mind that the TOPCon process included an inert annealing treatment around 900 °C that might allow gettering of contaminants, as suggested in [23,24].

4.2. Assessment of the lifetime level

An illustrative demonstration of the achieved material improvement is the reached lifetime level: the maxima of the τ_{eff} curves measured in Experiments 2 and 3 are among the highest lifetimes ever measured in crystalline silicon wafers of their respective doping concentration. This is illustrated in Fig. 6 via a comparison to literature data. The application of state-of-the-art passivation schemes on FZ wafers after proper pre-treatment shows that charge carrier lifetimes in moderately doped silicon have a higher potential than expected thus far. To our knowledge the τ_{eff} of 225 ms on the high resistivity n-type sample passivated with TOPCon is the highest lifetime ever measured in a crystalline silicon wafer (cf. [11,14,22,31]).

Fig. 6(b) demonstrates that several studies published lately report measured effective lifetimes that clearly exceed the parametrisation of intrinsic recombination by Richter et al. [26]. Besides a demonstration of the progress in silicon surface passivation optimization this indicates that some of the FZ samples included in the Richter parametrisation might have been affected by gown-in bulk defects. We suggest that such

defects should be deactivated by high temperature pre-treatments to allow for quantification of the actual intrinsic lifetime limit of silicon. This is further supported by the observation from Fig. 3(c) and (d) that the parametrisation not only underestimates the maximum lifetime but also does not fully describe the measured injection dependence of the lifetime in high injection.

An important consequence of this observation is that reported surface recombination velocities S_{eff} or saturation current densities J_0 based on the Richter et al. parametrisation [26] do not quantify surface recombination correctly. The common approach to determine S_{eff} or J_0 from τ_{eff} measurements on samples of a single thickness (see e.g. chapter 2 of [38] for an introduction) cannot provide precise results based on a flawed assumed τ_{intr}. Interestingly, it depends on the specific process sequence whether the impact of surface recombination has been overestimated (i.e. when τ_{bulk} was affected by unexpected defects) or underestimated (i.e. when the processes allowed τ_{bulk} to exceed $\tau_{intr,Richter}$). This issue appears to be most pronounced at n-type material doping ranges exceeding $2 \cdot 10^{15}$ cm^{-3}, e.g. [39]. It can be overcome with a new experimental assessment of intrinsic recombination. Such assessment is presented by Veith-Wolf et al. in this issue [40]. Given the necessarily experimental nature of such parametrisations we recommend to perform thickness variation experiments as suggested by Yablonovitch et al. [41] for physically sound quantification of surface recombination.

4.3. Comparison of the passivation schemes

Both investigated dielectric passivation schemes are known to feature a good chemical passivation in combination with field effect
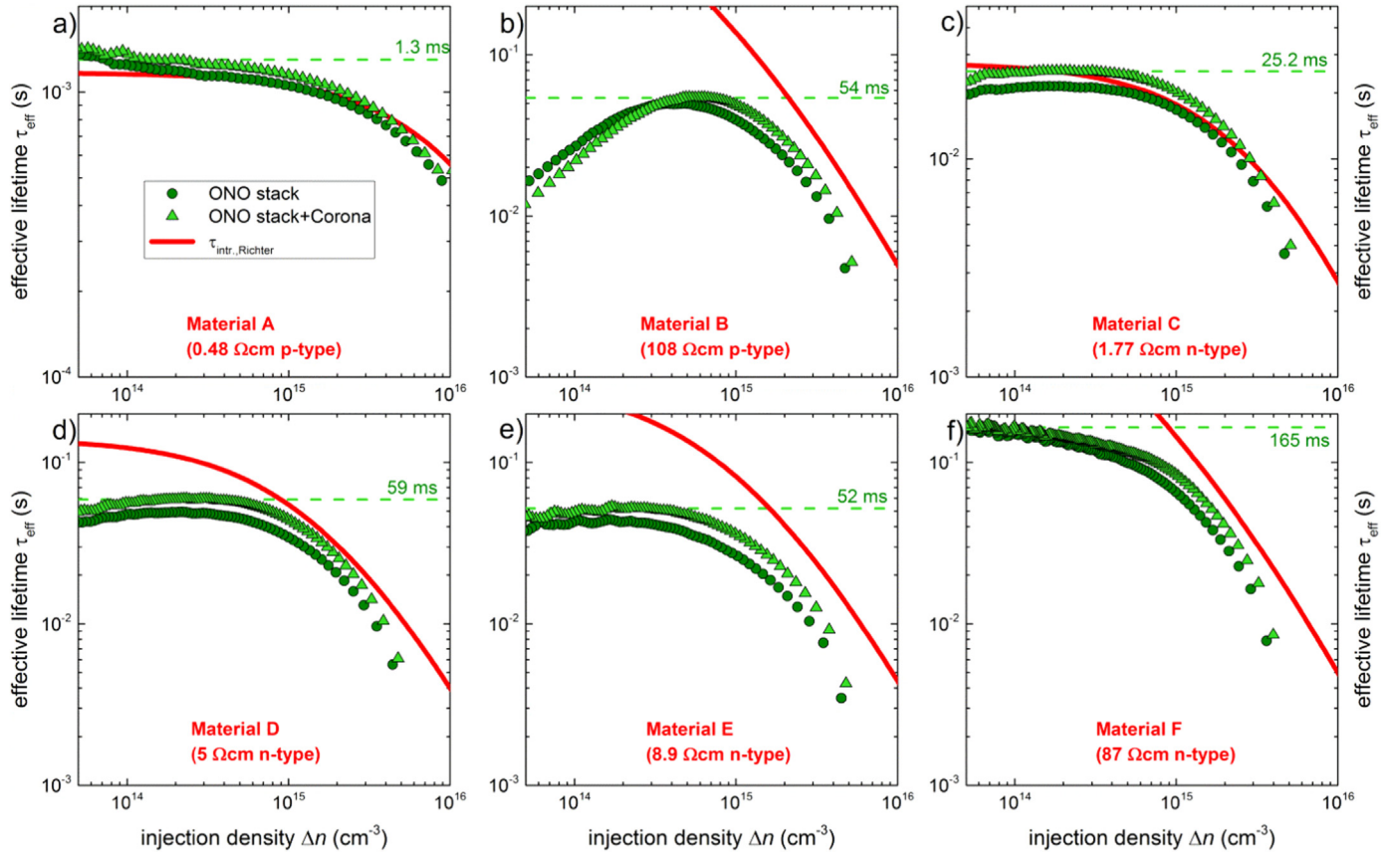
Fig. 4. Injection dependent τ_{eff} curves of the best samples of materials A-F passivated with the ONO stack (i.e. the same samples as shown in Fig. 3) before and after deposition of additional corona charge. The red solid lines denote the intrinsic lifetime limit parametrisation by Richter et al. [26] to aid comparison to Fig. 3. The dashed green lines indicate the extracted maximum lifetimes used for Fig. 6.
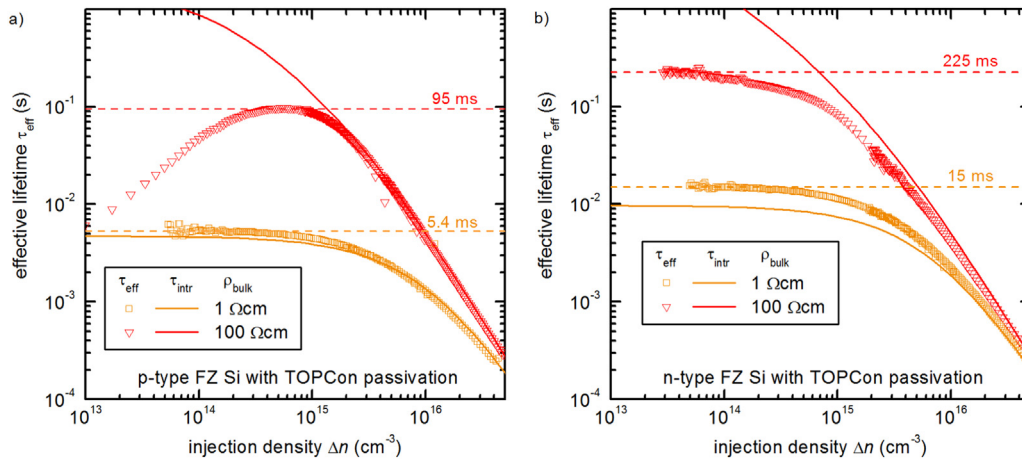

Fig. 5. Injection dependent τ_{eff} curves (transient mode for low injection, QSS mode with generalised evaluation [28] for high injection) of the best samples passivated with TOPCon layers. All samples feature record levels of τ_{eff} as indicated by the dashed lines. The results of the $1\,\Omega\,cm$ n-type sample (orange square symbols in b)) clearly exceeds the intrinsic lifetime limit parametrisation by Richter et al. [26] (solid lines) despite being uncorrected for surface recombination.

passivation caused by fixed charges (negative for Al_2O_3, positive for ONO) [14,42,43]. The direct comparison of the injection dependent τ_{eff} curves on the thermally pre-treated FZ materials allows for a direct comparison of the two investigated passivation schemes: the consistently better performance of Al_2O_3 passivation under high injection on both p- and n-type samples indicates that it features a lower interface trap density D_{it} than the ONO stack in this experiment. This observation is also valid when τ_{eff} of the Al_2O_3 passivated samples is compared to the ONO passivation after corona charging. This qualitative assessment is based on the consideration that surface recombination at high injection (i.e. when Δn is large so that $p_0 + \Delta n = p \approx n = n_0 + \Delta n$) is limited by the absolute concentration of

recombination sites that relates to D_{it}, while field effect passivation via fixed charges Q_f has a stronger impact at moderate Δn. This line of reasoning is restricted to strict high injection due to the asymmetric charge carrier capture cross sections at interface traps that can differ by orders of magnitude, e.g. [44,45]. In the given case of Experiment 2 the similar findings on p- and n-type samples can serve as supporting argument for a lower D_{it} of the investigated Al_2O_3 layers when compared to the ONO samples.

The low injection breakdown in passivation performance on material B for the ONO stack (see part b of Figs. 3 and 4) likely is a consequence of the strong component of field effect passivation via positive fixed charges. A similar trend is observed for the Al_2O_3 passivated
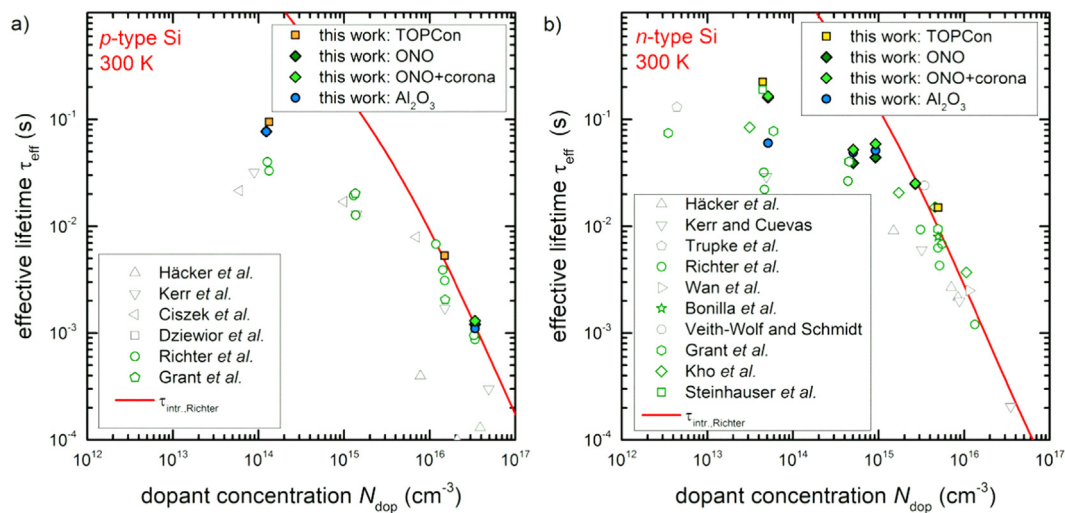
Fig. 6. Maxima of the best measured lifetime curves of the materials listed in Table 1 with several passivation schemes in comparison to literature data [11,14,17,22,26,31–37]: a) p-type materials, b) n-type materials.

sample of material F and was observed for similar samples, as well [26]. It could be caused by formation of an inversion layer acting as an effective conductive layer towards recombination centres, as suggested by Veith-Wolf et al. [18]. This agrees well with the observation that the breakdown of ONO was more pronounced and shifted towards higher injection after deposition of further positive charges (see Fig. 4(b)).

The respective samples prepared on Materials A, C, D & E are more likely affected by a Q_f-induced accumulation of minority charge carriers close to the surface, as their stronger doping might prevent the doping type change. A detailed investigation of this effect would require further doping concentrations and a large number of samples to reduce the impact of handling damage. It is beyond the scope of this work. The experiments demonstrate the general necessity of using optimised wafers (i.e. with stabilised τ_{bulk}) for fair direct comparison of different layers. This also includes studies that mention surface recombination velocity values or saturation current densities which could be distorted by the presence of bulk defects deactivated by certain process routes but not by others.

The different injection dependence found for high injection conditions in the measurement comparison at the different institutes shown in Fig. 3 was also observed for the sister samples. This systematic difference of the measured lifetime curves can be related to either systematic measurement artefacts or to changes of the measured samples between the measurements. A detailed investigation of this slight difference was beyond the scope of this work but the overall agreement of the measured τ_{eff} levels substantiates the validity of the high measured lifetimes.

5. Conclusion

In this contribution we have demonstrated that τ_{bulk} of typical commercially available FZ silicon wafers of various resistivities and both p- and n-type increases after commonly available thermal processes. We suggest a pre-treatment combining a POCl$_3$ diffusion step at 900 °C and a thermal oxidation treatment performed at 1050 °C to be applied prior to other experiments. This process sequence increases τ_{bulk} by deactivating or removing bulk defects that are often still present in the as-received state of state-of-the-art commercial wafers. Besides reducing the overall τ_{bulk} level of the wafer, these defects can distort experiments because they are affected by thermal treatments. The suggested combination of thermal treatments permanently deactivates these defects and the included POCl$_3$ diffusion allows for gettering of potentially present contaminants. The beneficial influence of the treatment has been demonstrated via the application of a superacid-

based passivation treatment that allows for an assessment of τ_{bulk} without significant thermal budget or incorporation of hydrogen.

The second part of the contribution demonstrated the excellent achieved quality of the pre-treated silicon wafers via passivation with high quality dielectric passivation schemes. The applied passivation schemes feature very different process routes and thermal budgets. The results demonstrate that excellent passivation properties were achieved with all passivation schemes. We present a direct comparison of two very different dielectric passivation schemes, permitted by stabilising the bulk material. Despite the small number of samples in the experiment, we can report record lifetimes on all investigated FZ materials. Outstanding effective lifetimes were achieved with the application of TOPCon layers to stabilised FZ Si wafers. We report τ_{eff} measured via transient photoconductance decay measurements of 225 and 15 ms on 200 μm thick 100 and 1 Ω cm n-type wafers, respectively.

The results shown and discussed in this contribution indicate that reported surface recombination velocities and parameterisations of intrinsic lifetime in the past were based on at least partially wrong assumptions. The effect is most pronounced for very good surface passivation schemes and should be taken into account for future assessments of surface recombination and intrinsic lifetime parameterisations.

assistance.

The authors are responsible for the content.

References

[1] F. Fertig, R. Lantzsch, A. Mohr, M. Schaper, M. Bartzsch, D. Wissen, F. Kersten, A. Mette, S. Peters, A. Eidner, J. Cieslak, K. Duncker, M. Junghänel, E. Jarzembowksi, M. Kauert, B. Faulwetter-Quandt, D. Meißner, B. Reiche, S. Geißler, S. Hörnlein, C. Klenke, L. Niebergall, A. Schönmann, A. Weihrauch, F. Stenzel, A. Hofmann, T. Rudolph, A. Schwabedissen, M. Gundermann, M. Fischer, J.W. Müller, D.J.W. Jeong, Mass production of p-type Cz silicon solar cells approaching average stable conversion efficiencies of 22%, Energy Procedia 124 (2017) 338–345.

[2] K. Yoshikawa, H. Kawasaki, W. Yoshida, T. Irie, K. Konishi, K. Nakano, T. Uto, D. Adachi, M. Kanematsu, H. Uzu, K. Yamamoto, Silicon heterojunction solar cell with interdigitated back contacts for a photoconversion efficiency over 26%, Nat. Energy 2 (5) (2017) 17032.

[3] M.A. Green, Y. Hishikawa, E.D. Dunlop, D.H. Levi, J. Hohl-Ebinger, A.W.Y. Ho-Baillie, Solar cell efficiency tables (version 51), Prog. Photovolt. Res. Appl. 26 (1) (2018) 3–12.

[4] Y.M. Yang, A. Yu, B. Hsu, W.C. Hsu, A. Yang, C.W. Lan, Development of high-performance multicrystalline silicon for photovoltaic industry, Prog. Photovolt.: Res. Appl. 23 (3) (2015) 340–351.

[5] A. Herguth, G. Hahn, Kinetics of the boron-oxygen related defect in theory and experiment, J. Appl. Phys. 108 (11) (2010) 114509.

[6] P. Hamer, B. Hallam, S. Wenham, M. Abbott, Manipulation of hydrogen charge states for passivation of P-type wafers in photovoltaics, IEEE J. Photovolt. 4 (5) (2014) 1252–1260.

[7] M.B. Shabani, T. Yamashita, E. Morita, Study of gettering mechanisms in silicon: competitive gettering between phosphorus diffusion gettering and other gettering sites, Solid State Phenom. 131–133 (2008) 399–404.

[8] N.E. Grant, V.P. Markevich, J. Mullins, A.R. Peaker, F. Rougieux, D. Macdonald, J.D. Murphy, Permanent annihilation of thermally activated defects which limit the lifetime of float-zone silicon, Phys. Status Solidi (a) 213 (11) (2016) 2844–2849.

[9] N.E. Grant, F.E. Rougieux, D. Macdonald, J. Bullock, Y. Wan, Grown-in defects limiting the bulk lifetime of p-type float-zone silicon wafers, J. Appl. Phys. 117 (5) (2015) 55711.

[10] N.E. Grant, V.P. Markevich, J. Mullins, A.R. Peaker, F. Rougieux, D. Macdonald, Thermal activation and deactivation of grown-in defects limiting the lifetime of float-zone silicon, Phys. Status Solidi-Rapid Res. Lett. 10 (6) (2016) 443–447.

[11] N.E. Grant, T. Niewelt, N.R. Wilson, E.C. Wheeler-Jones, J. Bullock, M. Al-Amin, M.C. Schubert, A.C. van Veen, A. Javey, J.D. Murphy, Superacid-treated silicon wafers: extending the limits of bulk and surface lifetimes for high efficiency photovoltaic devices, IEEE J. Photovolt. 7 (6) (2017) 1574–1583.

[12] L.J. van der Pauw, A method of measuring the resistivity and hall coefficient on lamellae of arbitrary shape, Philips Tech. Rev. 20 (1958) 220–224.

[13] A. Richter, J. Benick, M. Hermle, Boron emitter passivation with Al₂O₃ and Al₂O₃/SiNₓ stacks using ALD Al₂O₃, IEEE J. Photovolt. 3 (1) (2013) 236–245.

[14] T. Kho, K. Fong, K.R. McIntosh, E. Franklin, N.E. Grant, M. Stocks, S.P. Phang, Y. Wan, E.-.C. Wang, K. Vora, Z. Ngwe, A. Blakers, Exceptional silicon surface passivation by an ONO dielectric stack, Sol. Energy Mater. Sol. Cells (Submitted for publication), 2018.

[15] S. Kleekajai, L. Wen, C. Peng, M. Stavola, V. Yelundur, K. Nakayashiki, A. Rohatgi, J. Kalejs, Infrared study of the concentration of H introduced into Si by the post-deposition annealing of a SiNx coating, J. Appl. Phys. 106 (12) (2009) 123510.

[16] A.Y. Liu, C. Sun, V.P. Markevich, A.R. Peaker, J.D. Murphy, D. Macdonald, Gettering of interstitial iron in silicon by plasma-enhanced chemical vapour deposited silicon nitride films, J. Appl. Phys. 120 (19) (2016) 193103.

[17] B.A. Veith-Wolf, J. Schmidt, Unexpectedly high minority-carrier lifetimes exceeding 20 ms measured on 1.4-Ω cm n-type silicon wafers, Phys. Status Solidi-Rapid Res. Lett. 11 (11) (2017).

[18] B. Veith, T. Ohrdes, F. Werner, R. Brendel, P.P. Altermatt, N.-P. Harder, J. Schmidt, Injection dependence of the effective lifetime of n-type Si passivated by Al₂O₃: an edge effect? Sol. Energy Mater. Sol. Cells 120 (2014) 436–440.

[19] R.S. Bonilla, P.R. Wilshaw, On the c-Si/SiO2 interface recombination parameters from photo-conductance decay measurements, J. Appl. Phys. 121 (13) (2017) 135301.

[20] R.S. Bonilla, N. Jennison, D. Clayton-Warwick, K.A. Collett, L. Rands, P.R. Wilshaw, Corona charge in SiO2: kinetics and surface passivation for high efficiency silicon solar cells, Energy Procedia 92 (2016) 326–335.

[21] R.S. Bonilla, C. Reichel, M. Hermle, P. Hamer, P.R. Wilshaw, Long term stability of c-Si surface passivation using corona charged SiO2, Appl. Surf. Sci. 412 (2017) 657–667.

[22] B. Steinhauser, J.-I. Polzin, F. Feldmann, M. Hermle, S.W. Glunz, Excellent surface passivation quality on crystalline silicon using industrial-scale direct-plasma TOPCon deposition, Technol. Sol. RRL 142 (2018) 1800068.

[23] J. Krügener, F. Haase, M. Rienäcker, R. Brendel, H.J. Osten, R. Peibst, Improvement of the SRH bulk lifetime upon formation of n-type POLO junctions for 25% efficient Si solar cells, Sol. Energy Mater. Sol. Cells 173 (2017) 85–91.

[24] A. Liu, Di Yan, S.P. Phang, A. Cuevas, D. Macdonald, Effective impurity gettering by phosphorus- and boron-diffused polysilicon passivating contacts for silicon solar cells, Sol. Energy Mater. Sol. Cells 179 (2018) 136–141.

[25] S. Lindekugel, H. Lautenschlager, T. Ruof, S. Reber, Plasma hydrogen passivation for crystalline silicon thin-films, in: Proceedings of 23rd EU PVSEC, Valencia, 2008, pp. 2232–2235.

[26] A. Richter, S.W. Glunz, F. Werner, J. Schmidt, A. Cuevas, Improved quantitative description of Auger recombination in crystalline silicon, Phys. Rev. B 86 (16) (2012) 165202.

[27] T.C. Kho, S.C. Baker-Finch, K.R. McIntosh, The study of thermal silicon dioxide electrets formed by corona discharge and rapid-thermal annealing, J. Appl. Phys. 109 (5) (2011) 53108.

[28] H. Nagel, C. Berge, A.G. Aberle, Generalized analysis of quasi-steady-state and quasi-transient measurements of carrier lifetimes in semiconductors, J. Appl. Phys. 86 (11) (1999) 6218–6221.

[29] V.V. Voronkov, The mechanism of swirl defects formation in silicon, J. Cryst. Growth 59 (3) (1982) 625–643.

[30] A. Lenz, A. Huber, The impact of annealing steps on minority carrier lifetime of nitrogen co-doped FZ-crystals and correlating DLTS-defect-levels, in: ip.com.

[31] T. Trupke, R.A. Bardos, F. Hudert, P. Würfel, J. Zhao, A. Wang, M.A. Green, Effective excess carrier lifetimes exceeding 100 milliseconds in float zone silicon determined from photoluminescence, in: Proceedings of 19th EU PVSEC, Paris, 2004, pp. 758–761.

[32] Y. Wan, K.R. McIntosh, A.F. Thomson, A. Cuevas, Low surface recombination velocity by low-absorption silicon nitride on c-Si, IEEE J. Photovolt. 3 (1) (2013) 554–559.

[33] R.S. Bonilla, C. Reichel, M. Hermle, P.R. Wilshaw, Extremely low surface recombination in 1 Ω cm n-type monocrystalline silicon, Phys. Status Solidi RRL 11 (1) (2017) 1600307.

[34] T.F. Ciszek, T. Wang, T. Schuyler, A. Rohatgi, Some effects of crystal growth parameters on minority carrier lifetime in float-zoned silicon, J. Electrochem. Soc. 136 (1) (1989) 230–234.

[35] R. Häcker, A. Hangleiter, Intrinsic upper limits of the carrier lifetime in silicon, J. Appl. Phys. 75 (11) (1994) 7570–7572.

[36] M.J. Kerr, A. Cuevas, General parameterization of Auger recombination in crystalline silicon, J. Appl. Phys. 91 (4) (2002) 2473–2480.

[37] J. Dziewior, W. Schmid, Auger coefficients for highly doped and highly excited silicon, Appl. Phys. Lett. 31 (5) (1977) 346–348.

[38] L.E. Black, New perspectives on surface passivation: understanding the Si-Al2O3 interface (Dissertation). Canberra, Australia, 2016.

[39] A.I. Pointon, N.E. Grant, E.C. Wheeler-Jones, P.P. Altermatt, J.D. Murphy, Superacid-derived surface passivation for measurement of ultralong lifetimes in silicon photovoltaic materials, Sol. Energy Mater. Sol. Cells 183 (2018) 164–172.

[40] B.A. Veith-Wolf, S. Schäfer, R. Brendel, J. Schmidt, Reassessment of intrinsic lifetime limit in n-type crystalline silicon and implication on maximum solar cell efficiency, Sol. Energy Mater. Sol. Cells (Submitted for publication), 2018.

[41] E. Yablonovitch, D.L. Allara, C.C. Chang, T. Gmitter, T.B. Bright, Unusually low surface-recombination velocity on silicon and germanium surfaces, Phys. Rev. Lett. 57 (2) (1986) 249–252.

[42] R.S. Bonilla, B. Hoex, P. Hamer, P.R. Wilshaw, Dielectric surface passivation for silicon solar cells: a review, Phys. Status Solidi (a) 214 (7) (2017) 1862–6319.

[43] A. Richter, J. Benick, A. Kimmerle, M. Hermle, S.W. Glunz, Passivation of phosphorus diffused silicon surfaces with Al2O3: influence of surface doping concentration and thermal activation treatments, J. Appl. Phys. 116 (24) (2014) 243501.

[44] R.B.M. Girisch, R.P. Mertens, R.F. de Keersmaecker, Determination of Si-SiO₂ interface recombination parameters using a gate-controlled point-junction diode under illumination, IEEE Trans. Electron Devices 35 (2) (1988) 203–222.

[45] D. Schuldis, A. Richter, J. Benick, P. Saint-Cast, M. Hermle, S.W. Glunz, Properties of the c-Si/Al2O3 interface of ultrathin atomic layer deposited Al2O3 layers capped by SiNx for c-Si surface passivation, Appl. Phys. Lett. 105 (23) (2014) 231601.